RESEARCH ARTICLE

Journal of
Orthopaedic
Research®

Feasibility of aluminum phantom radiography for osteoporosis detection in postmenopausal women with a fragility fracture of the distal radius compared to DXA and HR-pQCT

Arastoo Nia[1] 🄾 | Natasa Jeremic[1] 🄾 | Domenik Popp[1] 🄾 | Lukas Schmoelz[1] 🄾 |
Janina Patsch[2] 🄾 | Kevin Döring[1] 🄾 | Michael Weber[2] 🄾 | Alexander Synek[3] 🄾 |
Dieter H. Pahr[3,4] 🄾 | Silke Aldrian[1]

[1]Department of Orthopedics and Trauma Surgery, Division of Trauma Surgery, Medical University of Vienna, Vienna, Austria

[2]Department of Biomedical Imaging and Image-guided Therapy, Medical University of Vienna, Vienna, Austria

[3]Institute of Lightweight Design and Structural Biomechanics, TU Wien, Wien, Austria

[4]Division Biomechanics, Karl Landsteiner University of Health Sciences, Krems an der Donau, Austria

Correspondence
Arastoo Nia, Department of Orthopedics and Trauma Surgery, Division of Trauma Surgery, Medical University of Vienna, Währinger Straße 18-20, 1090 Vienna, Austria.
Email: arastoo.nia@meduniwien.ac.at

Abstract

Recently, promising results have been reported for detection of osteoporosis with use of an aluminum phantom. Therefore, the aim of this study was to evaluate the feasibility of radiography-based bone mineral density (BMD) measurement using a graded aluminum phantom. This study included 27 postmenopausal women with a distal radius fracture. Aluminum phantom radiography of the healthy radius was conducted as well as high-resolution peripheral quantitative computed tomography (HR-pQCT) measurement of the ultradistal radius and dual energy X-ray absorptiometry (DXA) of the radius, spine, and hip. A strong correlation was observed between aluminum phantom radiography-based mean gray value (mGV) and DXA-derived BMD, especially for the ultradistal radius ($\rho = 0.75$; $p < 0.001$). A moderate correlation for the femoral neck ($\rho = 0.61$ and $p < 0.001$) between modalities was found. Radius mGV and HR-pQCT-derived BMD only showed a moderate correlation ($\rho = 0.48$; $p < 0.09$). Aluminum phantom radiography might serve as a cost efficient, highly available, low-radiation dose screening, and diagnostic method for osteoporosis additively to DXA measurements. Especially, an application in areas with constrained DXA availability and such as preoperative trauma settings would be beneficial. However, further investigation and assessment of specificity and sensitivity is needed.

KEYWORDS
aluminum phantom, bone mineral density, DXA, HR-pQCT, osteoporosis

1 | INTRODUCTION

Several different techniques for the measurement of bone mineral density (BMD) are available, including dual energy X-ray absorptiometry (DXA), which is the gold standard and most commonly used method.[1,2] Recently, radiographic absorptiometry has been a subject of research, particularly in the field of osteoarthritis.[3]

Prior studies measuring BMD using digital X-ray and aluminium phantoms showed strong correlations in BMD changes in knee

radiographs of osteoarthritis patients.[4] The radiation exposure and the image processing must, however, be carried out carefully and in a standardized manner to achieve accurate results. X-ray settings, including tube voltage (measured in kilovolts, kV) and exposure (measured in milliampere seconds, mAs) often vary between devices, which may influence BMD results. Therefore, image postprocessing is incorporated in the scan protocol, which includes contrast adjustment curves and applications of nonlinear image filters to optimize image quality parameters such as contrast and noise.[5] Image postprocessing aims to improve diagnostic readability, rather than allowing quantitative analyses to assess BMD changes for longitudinal evaluation.[4] With addition of the Greyscale phantom (GS), such as the inclusion of an aluminum step wedge in the radiographic field-of-view, as suggested by Hirvasniemi et al.,[6] the influence of postprocessing is minimized. Additionally, by using an aluminum phantom, the gray values (GV) of the bone can be expressed in millimeter aluminum equivalents (mmAl), which allows for BMD to be measured. This GS model thus may reduce time, costs, and patient radiation exposure due to a potential fusion of radiography and BMD measurement.[7]

The aim of this study was therefore to measure and correlate BMD in female patients with a recent fragility fracture using digital X-rays. To evaluate the applicability of BMD measurements in clinical practice and research application, this method was compared with DXA and high-resolution peripheral quantitative computed tomography (HR-pQCT) measurements.

2 | MATERIALS AND METHODS

2.1 | Study design and setting

This prospective pilot study included all postmenopausal women who experienced a low-energy fracture (defined as the equivalent to falling from a standing height or less) admitted to a Level 1 trauma center during the period of December 1, 2021 to December 31, 2021. Patients who had the following conditions affecting bone mass, such as prior or current treatment for osteoporosis, severe renal or liver disorder, intake of glucocorticoids, antacids, testosterone supplements, rosiglitazone, pioglitazone, steroid hormones, anticonvulsants, and anticoagulants, were excluded.

A total of 27 patients met the criteria mentioned above and were included in the study. The mean age was 60.3 years, ±6.7 SD. The mean weight was 67.8 kg, ±12.3 SD (range 49–90), the mean body mass index was 24.4 kg/m^2, ±4.1 SD (range 20–32), and the mean height was 166.8 cm, ±6.1 SD (range 157–176).

As illustrated in the graphical abstract (Figure 1), first an additional anterior posterior (AP) and lateral digital radiography of the contralateral radius was performed with an aluminum step wedge placed at the side of the wrist. Both DXA and HR-pQCT scans of the same region were used to validate the radiographic-based BMD measurement. All radiographic scans were performed at the same visit.

DXA measurement of areal BMD was assessed at the spine, hip, and distal part of the nonfractured forearm using the Discovery DXA scanner (Hologic Inc.) according to standard protocol.[8,9] For analyses, osteoporosis was defined as a t score of −2.5 SD using the World Health Organization criteria.

HR-pQCT (XtremeCT I- SCANCO Medical AG) was performed of the nondominant, nonfractured radius and the tibia. The image acquisition and analysis of a 9 mm stack of the ultradistal radius and tibia scan were performed using the standard built-in software (XtremeCT, version 6.0). The scanning methodology has previously been described.[10,11] A single stack of parallel computer tomography (CT) slices (110 slices = 9.02 mm) for each site was acquired in the high-resolution mode (image matrix = 1536 × 1536, Isotropic voxel sizes of 82 μm). Daily measurements of the manufacturer device-specific phantom (Scanco Medical AG) were performed for quality control.

3 | RADIOGRAPHY WITH GRADED ALUMINUM PHANTOM

The default clinical radiography protocol was used as provided by the manufacturer (Philips bucky DIAGNOST X-Ray). The mean voltage used for the radiographs was 49.3 kV, ±4.0 SD. The mean tube current was 2.1 mAs, ±0.5 SD. A GS (Figure 2), which is an aluminum staircase, was manufactured in-house, which has various steps and was used for conversion of GV in mmAl. The height of these steps corresponds to a height of 1–4, 5–8, 9–11, and 12–14 mm, and are used as a reference for image calibration. The first two steps (1–8 mm) were used in this study. For X-ray acquisition, the patient's forearm was positioned in a custom-designed and three-dimensionally printed hand splint. It was used during AP and lateral radiography. A special marker within the hand fixation was used as a reference point for positioning. To quantify BMD and to determine the pixel size corrected for possible magnification, the aluminum phantom was placed alongside the radius, against the detector, and within the field of exposure.

X-ray images were then preprocessed and converted into a MetaImage or mhd file format for further evaluation. After calibration, the calculation of the mGV was performed by using medtool 4.5 software (Dr. Pahr Ingenieurs e.U.). The definition of the region of interest (ROI) of each X-ray image was equivalent to that of the HR-pQCT and DXA, to ensure the most accurate comparison of values. The dorsal radial tuberosity was used as a point of reference. A 9 mm-long ROI was defined below it. To refine the calculation and attain more accurate values, an additional segmentation of the image was performed. This allowed the subtraction of the hypodense background to evaluate the bony structures more precisely. The mGV of the image was calculated in mmAl, which is equivalent to the two-dimensional BMD.

4 | STATISTICAL AND BIOMETRIC EVALUATION

After checking the data for normal distribution using histograms and QQ plots, Spearman's linear rank correlation analysis was performed to test for correlation, as there was no normal distribution of the data.
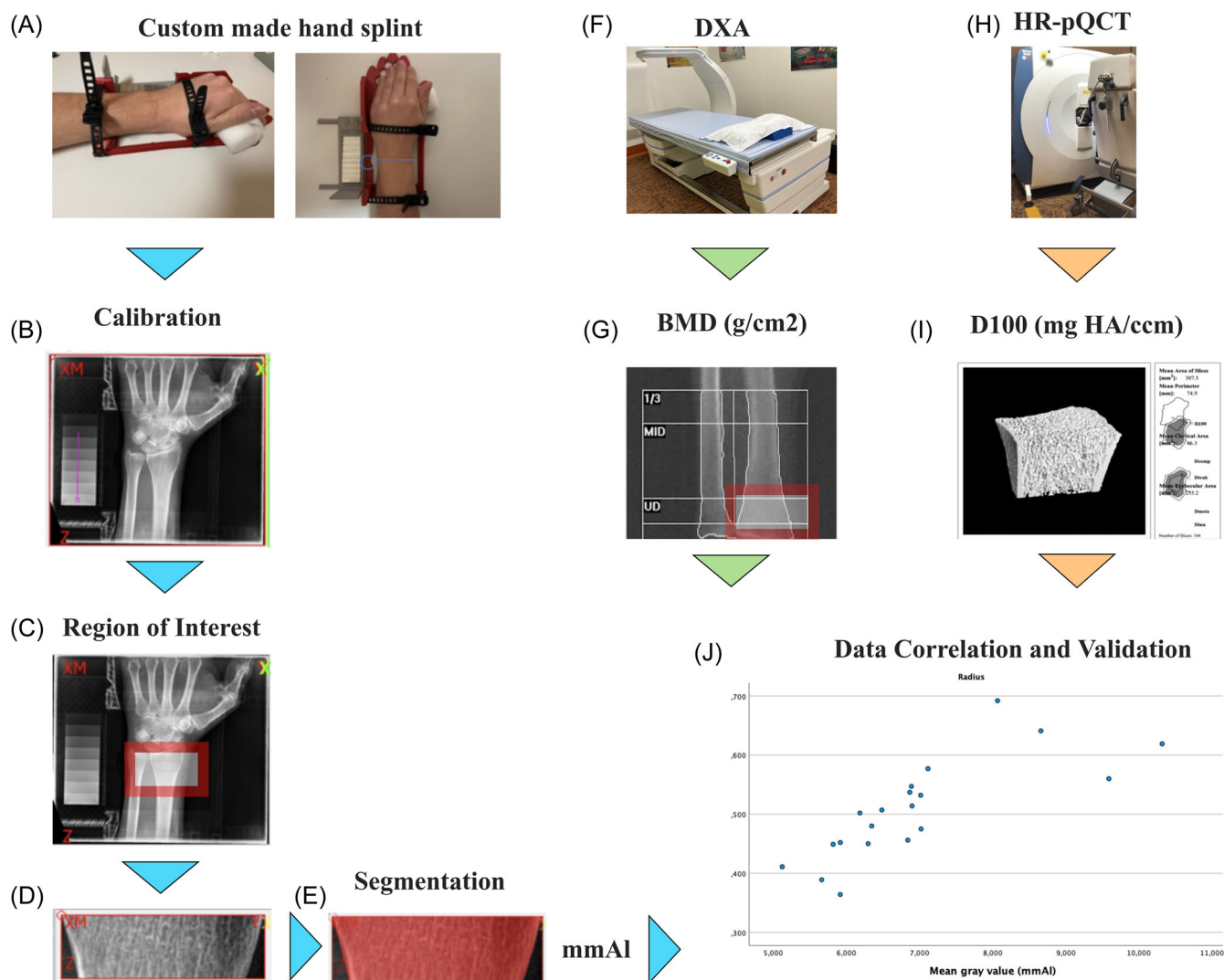
FIGURE 1 Graphical abstract of the project. Twenty-seven patients underwent radiographic (A), dual energy X-ray absorptiometry (DXA) (F), and high-resolution peripheral quantitative computed tomography (Hr-pQCT) (H) scanning of the radius to determine bone mineral density (BMD). Calibration (B) and definition of region of interest (ROI) (C), which was equivalent to that of the Hr-pQCT (I) and DXA (G). Furthermore, an additional segmentation with subtraction of the hypodense background was performed (D, E). The correlation between mean gray value- (mGV), DXA-, and Hr-pQCT-derived BMD was evaluated statistically (J).
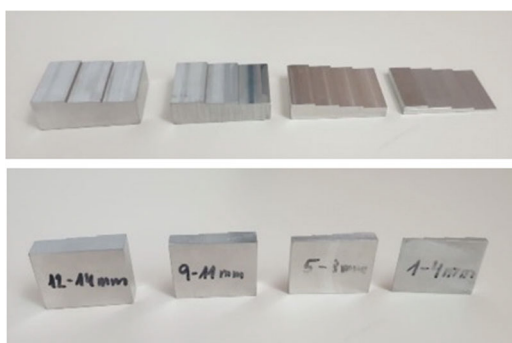

FIGURE 2 The Greyscale phantom, an aluminum staircase of various degrees of density.

The lack of a normal data distribution can potentially be attributed to the small number of patients in this study. As Pearson's correlation analysis was performed in the literature for similar studies, it was used in our work to avoid erroneous comparisons between our rank-based correlation coefficients and nonrank-based correlation coefficients of other studies. Both correlation coefficients have a rank range from −1 to 1. A positive correlation with a correlation coefficient of >0.8 is considered excellent. The calculation of the cutoff values, based on the mGV, for the classification of the patients into healthy and osteoporotic was performed by reference to the lowest BMD in each case. Accordingly, ordinal regression was used to test the success of assignment to each group. The significance level was set at $p < 0.05$ for all analyses. Statistical analyses were performed using SPSS (Statistical Package for the Social Sciences) 15.0 software.

5 | RESULTS

Spearman's correlation analysis showed moderate to strong two-sided correlations of the aluminum phantom radiography-based mGV values and DXA-derived t scores. The strongest correlation was found at the radius ($\rho = 0.75$, $p < 0.001$) and the weakest was at the lumbar spine ($\rho = 0.54$, $p < 0.004$), whereas a moderate correlation was observed at the femoral neck ($\rho = 0.61$ and $p < 0.001$; Table 1).

Spearman's correlation analyses of mGV- and DXA-derived BMD showed a strong correlation at the lumbar spine ($\rho = 0.62$, $p < 0.001$), a moderate correlation at the femoral neck ($\rho = 0.51$, $p < 0.007$) and an excellent correlation at the radius ($\rho = 0.89$, $p < 0.001$; Table 1 and Figure 3).

An excellent correlation was found between mGV and the t score of the femoral neck ($r = 0.83$, $p < 0.001$). Good correlation coefficients were found between mGV and the t score of radius ($r = 0.75$, $p < 0.001$) and lumbar spine ($r = 0.74$, $p < 0.001$; Table 2).

Similar results were found between mGV- and DXA-derived BMD of the lumbar spine ($r = 0.73$, $p < 0.001$) and radius ($r = 0.78$,

$p < 0.001$) in Pearson's correlation analysis. For femoral BMD, the analysis yielded a correlation coefficient of 0.59 and $p < 0.001$ (Table 2 and Figure 4).

Spearman's correlation analysis showed moderate to poor correlation between HR-pQC-derived total volumetric BMD (D100) and mGV. The correlation coefficient between mGV and D100 was $\rho = 0.33$ at the radius ($p < 0.09$) and $\rho = 0.48$ at the tibia ($p < 0.012$) (Table 3).

When considering HR-pQCT parameters and mGV together, a moderate correlation was seen in Pearson's correlation analysis. Interestingly, the tibial values showed similarly high correlation coefficients (Table 3 and Figure 5).

Regarding group allocation, 11 of the 14 patients (79%) were correctly assigned to the osteopenia group and 6 of the 10 (60%) osteoporotic patients to the osteoporosis group. All 24 patients with reduced BMD (osteopenia or osteoporosis) were assigned to one of the two groups (Table 4).

6 | DISCUSSION

Due to socioeconomic reasons and availability, measuring BMD might be feasible on plain digital radiographs in clinical practice. The method depicted in our study represents a potential osteoporosis detection tool with high availability, low costs, and low radiation exposure. Due to the information gained with this study, treating clinicians could consider using this easily applicable method in the preoperative setting for estimation of BMD from digital radiographs.

Recently, Robertson et al.[7] measured 13 male and female patients and showed a strong correlation of aluminum equivalent measurements with DXA-derived regions. This research used a Pearson's correlation coefficient model and showed strong correlations for aluminum equivalent forearm DXA values ($r = 0.64$), comparing the fractured and not fractured arm,[7] and they found weak correlations for hip DXA values ($r = 0.33$). Our study also showed strong correlations, but are not directly comparable as the

TABLE 1 Spearman–ρ correlation of DXA values with mGV of aluminum phantom radiography.

	ρ	Sig. (two-sided)	n
T-Score/mGV			
Lumbar spine	0.54	0.004	27
Femoral neck	0.61	0.001	27
Radius	0.75	0.001	27
BMD/mGV			
Lumbar spine	0.62	0.001	27
Femoral neck	0.51	0.007	27
Radius	0.89	0.001	27

Abbreviations: BMD, bone mineral density; DXA, dual energy X-ray absorptiometry; mGV, mean gray value.

FIGURE 3 Relationship of dual energy X-ray absorptiometry (DXA) derived bone mineral density (BMD) values of femoral neck and the mean gray value (mGV). The uphill pattern shows a positive linear relation between both continuous variables.
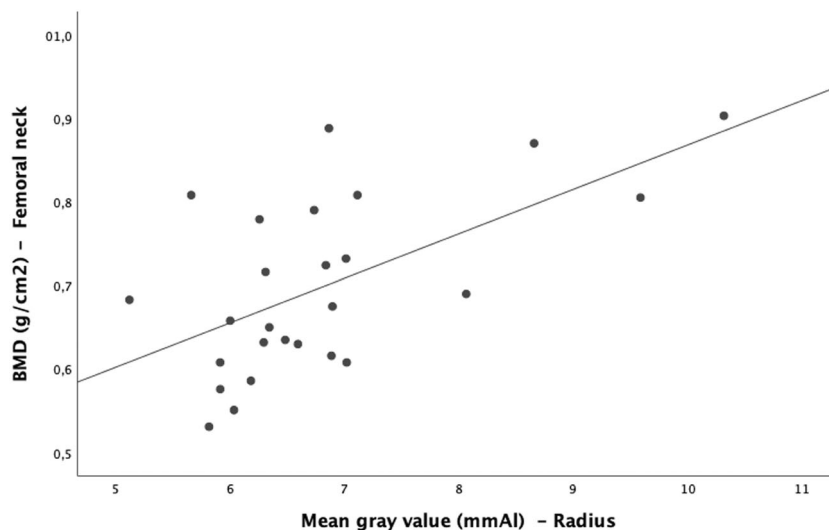
Spearman–ρ correlation coefficients were more suitable in our study due to the lack of normal distribution of data. Furthermore, the date of the measurements of the fractured forearm is crucial, as any immobilization leads to significant changes in BMD and bone microarchitecture.[12]

Webber et al.[13] also examined AP radiographs of patients with radius fractures and attempted to obtain information about BMD based on the cortical thickness of the distal radius. They showed that cortical thickness correlated moderately with BMD of the proximal femur ($\rho = 0.44$; $p < 0.01$), but not with the lumbar spine, which is in general not well suited for cortical bone measurements. This may be explained by differences in bone structure. Due to differences in force application and distribution, the vertebral bodies have higher cancellous fraction than in long bones.[13]

However, the present study results could not confirm this. Although the Spearman–ρ correlation for mGV in the hip region was slightly stronger than in the lumbar spine region when the t score was analyzed, a negative correlation was seen regarding the BMD. The same applies for Pearson's correlation analysis, where we obtained an excellent correlation coefficient for the femoral t score. A possible reason for this could be that some authors, such as Webber et al.[13] analyzed only the cortical aspect of the bone (cortical thickness) when analyzing the BMD of the lumbar spine. It is also possible that the results could have been influenced by the fact that the fractured side was always measured.

According to Vaccaro et al.,[14] a BMD drop of at least 30%–40% must be present to detect it on radiography. Accordingly, some borderline osteoporotic patients should be undetected and classified as false-healthy on radiography-blinded screening. In our analyses, this assumption was not confirmed. Most importantly, no patient was misclassified as healthy. Aluminum phantom radiography detected all 24 patients with decreased BMD. However, there seems to be inaccuracies in the differentiation between osteopenia and osteoporosis. Furthermore, it should be mentioned that there were only three patients with normal BMD in our study. Additive methods in addition to mean gray level determination, such as bone texture analysis using neural networks, would be an interesting way to increase the accuracy of the measurement and further improve the classification if necessary.

In an ex vivo study, Hirvasniemi et al.[15] found a strong correlation of micro-CT parameters and radiographic measurement using GS. However, we are not aware of any study comparing the procedure with HR-pQCT. The moderate correlation of D100 with mGV ($\rho < 0.476$ and $\rho < 0.333$)

TABLE 2 Pearson's correlation of DXA values with mGV of aluminum phantom radiography.

	Pearson's correlation	Sig. (two-sided)	n
T-Score/mGV			
Lumbar spine	0.74	<0.001	27
Femoral neck	0.83	<0.001	27
Radius	0.75	<0.001	27
BMD/mGV			
Lumbar spine	0.73	<0.001	27
Femoral neck	0.59	<0.001	27
Radius	0.78	<0.001	27

Abbreviations: BMD, bone mineral density; DXA, dual energy X-ray absorptiometry; mGV, mean gray value.

TABLE 3 Spearman–ρ correlation of HR-pQCT and mGV of aluminum phantom radiography.

HR-pQCT/mGV	ρ	Sig. (two-sided)	n
D100 Radius	0.33	0.09	27
D100 Tibia	0.48	0.012	27

Abbreviations: HR-pQCT, high-resolution peripheral quantitative computed tomography; mGV, mean gray value.
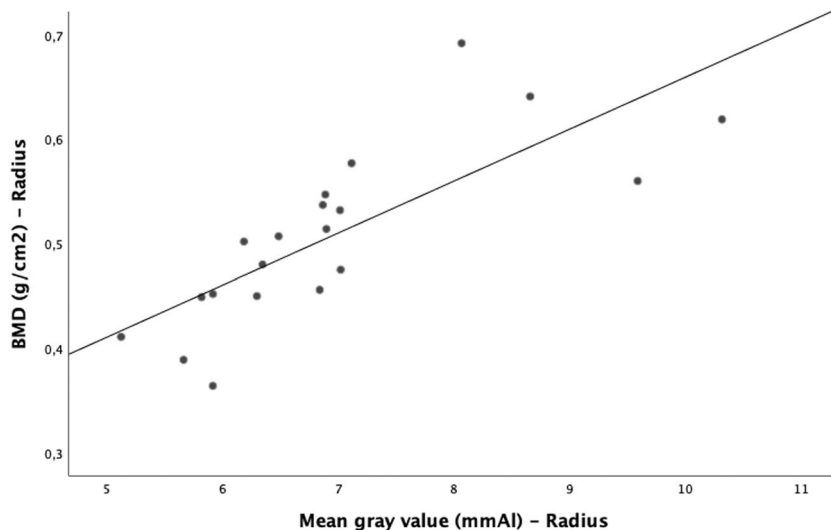

FIGURE 4 Scatter plot of dual energy X-ray absorptiometry (DXA)-derived bone mineral density (BMD) values of radius and mean gray value (mGV).

FIGURE 5 Scatter plot of high-resolution peripheral quantitative computed tomography (HR-pQCT)-derived bone mineral density (BMD) values of radius and mean gray value (mGV).
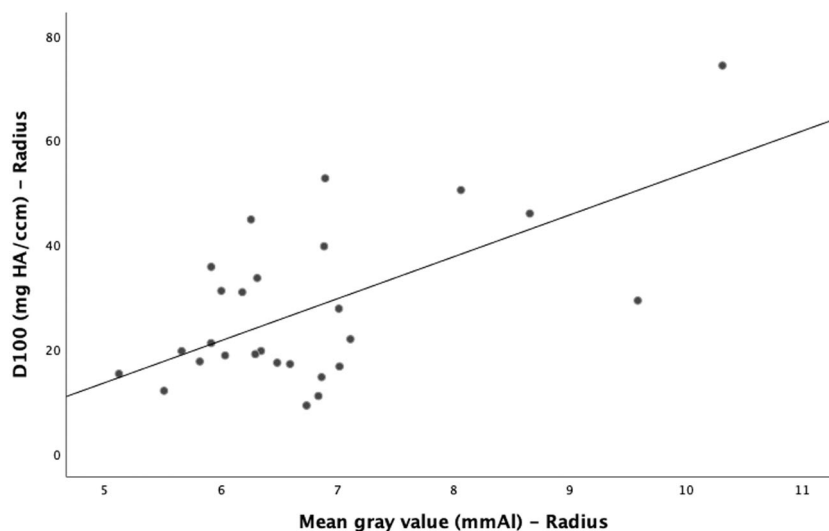

TABLE 4 Group allocation according to WHO classification based on the mGV.

T-Score		mGV prediction			
		$T > -1$	$T > -2.5$ and ≤ -1	$T \leq -2.5$	Total
$T > -1$	n (%)	3 (100%)	0	0	3
$T > -2.5$ and ≤ -1	n (%)	0	11 (79%)	3 (21%)	14
$T \leq -2.5$	n (%)	0	4 (40%)	6 (60%)	10
Total	n (%)	3 (11%)	15 (56%)	9 (33%)	27

Abbreviations: mGV, mean gray value; WHO, World Health Organization.

found in our data can be put into perspective by the partially moderate correlation of DXA values with HR-pQCT values ($\rho < 0.3$) for femoral BMD. Slightly stronger correlations for radius and lumbar spine BMD were observed in our study ($\rho < 0.7$). Amstrup et al.[16] showed only moderate correlations in some cases when comparing DXA, HR-pQCT, and QCT values, especially when comparing peripheral and central measurement regions. This could be explained by the fact that three dimensionality and measurement position play important roles.[17] However, as DXA is the gold standard for the diagnosis of osteoporosis, we primarily refer to the correlation of mGV with BMD values and t scores derived by DXA in our study.

7 | LIMITATIONS

There are several limitations of the present study. The possibility of measurement errors due to positioning was reduced through standardized positioning using a custom-made splint, but systematic errors cannot be completely excluded. Overall, this was a pilot study that examined a relatively small but homogeneous cohort. Although this does not affect the correlation analysis itself, it could be interesting to examine whether the method is similarly applicable in male patients. The number of osteoporotic patients cannot be extrapolated to the population due to the small number of cases and the selected sample group, especially because we excluded female patients with known osteoporosis in advance.

Aluminum phantom radiography might serve as a cost efficient, highly available, low-radiation dose screening, and diagnostic method for osteoporosis additively to DXA measurements. Specifically, its application in primary care and in areas with constrained DXA availability would be beneficial. Further studies with a larger number of cases and in a healthy population are necessary to determine the sensitivity and specificity of this potential risk assessment tool.

AUTHOR CONTRIBUTIONS

Arastoo Nia, Dieter H. Pahr, Alexander Synek, and Silke Aldrian contributed to conception and design of this study. Arastoo Nia, Natasa Jeremic, Lukas Schmoelz, Kevin Döring, and Domenik Popp contributed to the analysis of data. Dieter H. Pahr, Alexander Synek, Natasa Jeremic, and Michael Weber contributed to the interpretation of data. Article drafts were written by Arastoo Nia and critically revised by all authors.

CONFLICT OF INTEREST STATEMENT

The authors declare no conflict of interest.

ETHICS STATEMENT

This study was approved by the medical ethical review committee of the Medical University of Vienna (protocol number 2124/2019). All patients gave written informed consent. The procedures followed

were in accordance with the Helsinki Declaration of 1975, as revised in 2000.

ORCID

Arastoo Nia http://orcid.org/0000-0002-9001-7732

Natasa Jeremic http://orcid.org/0000-0003-2639-3060

Domenik Popp http://orcid.org/0000-0002-8580-2314

Lukas Schmoelz http://orcid.org/0000-0001-6455-0464

Janina Patsch http://orcid.org/0000-0002-5936-5608

Kevin Döring http://orcid.org/0000-0001-5982-5750

Michael Weber http://orcid.org/0000-0002-8507-2219

Alexander Synek http://orcid.org/0000-0002-5253-7403

Dieter H. Pahr http://orcid.org/0000-0002-5822-2082

REFERENCES

1. Kleerekoper M, Nelson DA, Flynn MJ, Pawluszka AS, Jacobsen G, Peterson EL. Comparison of radiographic absorptiometry with dual-energy X-ray absorptiometry and quantitative computed tomography in normal older White and black women. *J Bone Miner Res*. 2009;9:1745-1749. doi:10.1002/jbmr.5650091111

2. Kleerekoper M, Nelson DA, Peterson EL, et al. Reference data for bone mass, calciotropic hormones, and biochemical markers of bone remodeling in older (55-75) postmenopausal White and Black women. *J Bone Miner Res*. 2009;9:1267-1276. doi:10.1002/jbmr.5650090817

3. Arokoski JPA, Arokoski MH, Jurvelin JS, Helminen HJ, Niemetukia LH, Kroger H, et al. Increased bone mineral content and bone size in the femoral neck of men with hip osteoarthritis. *Ann Rheum Dis*. 2002;61:145-150. doi:10.1136/ARD.61.2.145

4. Kinds MB, Bartels LW, Marijnissen ACA, et al. Feasibility of bone density evaluation using plain digital radiography. *Osteoarthritis Cartilage*. 2011;19:1343-1348.

5. Buckland-Wright JC, Wolfe F, Ward RJ, Flowers N, Hayne C. Substantial superiority of semiflexed (MTP) views in knee osteoarthritis: a comparative radiographic study, without fluoroscopy, of standing extended, semiflexed (MTP), and schuss views. *J Rheumatol*. 1999;26:2664-2674.

6. Tiulpin A, Thevenot J, Hirvasniemi J, Niinimäki J, Saarakkala S. Acoustic emissions and kinetic instability as new clinical biomarkers to noninvasively assess knee osteoarthritis. *Osteoarthritis Cartilage*. 2018;26:S40-S41. doi:10.1016/j.joca.2018.02.097

7. Robertson G, Wallace R, Simpson AHRW, Dawson SP. Preoperative measures of bone mineral density from digital wrist radiographs. *Bone Joint Res*. 2021;10:830-839. doi:10.1302/2046-3758.1012.BJR-2021-0098.R1/ASSET/IMAGES/LARGE/BJR-2021-0098.R1-GALLEYFIG7.JPEG

8. Kanis JA, Melton LJ, Christiansen C, Johnston CC, Khaltaev N. The diagnosis of osteoporosis. *J Bone Miner Res*. 1994;9:1137-1141.

9. Blake GM, Fogelman I. Technical principles of dual energy X-ray absorptiometry. *Semin Nucl Med*. 1997;27:210-228. doi:10.1016/s0001-2998(97)80025-6

10. Boutroy S, Bouxsein ML, Munoz F, Delmas PD. In vivo assessment of trabecular bone microarchitecture by high-resolution peripheral quantitative computed tomography. *J Clin Endocrinol Metab*. 2005;90:6508-6515.

11. Patsch JM, Burghardt AJ, Kazakia G, Majumdar S. Noninvasive imaging of bone microarchitecture. *Ann NY Acad Sci*. 2011;1240:77-87.

12. Houde JP, Schulz LA, Morgan WJ, et al. Bone mineral density changes in the forearm after immobilization. *Clin Orthop Relat Res*. 1995;317:199-205.

13. Webber T, Patel SP, Pensak M, Fajolu O, Rozental TD, Wolf JM. Correlation between distal radial cortical thickness and bone mineral density. *J Hand Surg [Am]*. 2015;40:493-499.

14. Vaccaro C, Busetto R, Bernardini D, Anselmi C, Zotti A. Accuracy and precision of computer-assisted analysis of bone density via conventional and digital radiography in relation to dual-energy x-ray absorptiometry. *Am J Vet Res*. 2012;73:381-384.

15. Hirvasniemi J, Thevenot J, Kokkonen HT, et al. Correlation of subchondral bone density and structure from plain radiographs with micro computed tomography ex vivo. *Ann Biomed Eng*. 2016;44:1698-1709.

16. Amstrup AK, Jakobsen NFB, Moser E, Sikjaer T, Mosekilde L, Rejnmark L. Association between bone indices assessed by DXA, HR-pQCT and QCT scans in post-menopausal women. *J Bone Miner Metab*. 2016;34:638-645.

17. MacNeil JA, Boyd SK. Accuracy of high-resolution peripheral quantitative computed tomography for measurement of bone quality. *Med Eng Phys*. 2007;29:1096-1105.